Supplementary Information

Orally bioavailable and blood-brain barrier penetrating ATM inhibitor (AZ32) radiosensitizes intracranial gliomas in mice

Jeremy Karlin[1, #], Jasmine Allen[1, #], Syed F. Ahmad[1], Gareth Hughes[2], Victoria Sheridan[2], Rajesh Odedra[2], Paul Farrington[2], Elaine Cadogan[2], Lucy Riches[2], Antonio Garcia-Trinidad[2], Andrew Thomason[2], Bhavika Patel[2], Jennifer Vincent[2], Alan Lau[2], Kurt G. Pike[2], Tom Hunt[2], Amrita Sule[1], Nicholas C.K. Valerie[1], Laura Biddlestone-Thorpe[1], Jenna Kahn[1], Jason M. Beckta[1], Nitai D. Mukhopadhyay[1],Bernard Barlaam[2], Sebastien Degorce[2], Jason Kettle[2], Nicola Colclough[2], Joanne Wilson[2], Aaron Smith[2], Ian Barrett[2], Li Zheng[2], Tianwei Zhang[2], Yingchun Wang[2], Kan Chen[2], Martin Pass[2], Stephen T. Durant[2], and Kristoffer Valerie[1,*]

[1] Department of Radiation Oncology - Massey Cancer Center, Virginia Commonwealth University, Richmond, Virginia, USA

[2]AstraZeneca - Bioscience, DMPK, Chemistry, Discovery Sciences and Global IP – Oncology innovative Medicines (iMED) - Alderley Park, Macclesfield, Cheshire SK10 4TG, CRUK Cambridge Institute & Darwin Milton Science Park, Cambridge, UK, and Innovation Centre China, AstraZeneca, Shanghai, China

[#]*These authors contributed equally to this work.*

Running title: Novel orally bioavailable ATM inhibitor radiosensitizes glioma

[*] **Corresponding Author:** Kristoffer Valerie, Department of Radiation Oncology-Massey Cancer Center, Virginia Commonwealth University, VA, 23298-0058. Phone: 804-628-1004; FAX: 804-827-0635; Email: kristoffer.valerie@vcuhealth.org

Supplementary Methods

Kinase assays. In vitro and in vivo cell kinase assays were carried out as described previously (1), and references 12-14 therein.

Pharmacokinetics and efflux assays. MDCK-MDR1 Assay. Permeability (P_{app}) and the efflux ratio of compounds were determined using human MDCK cells expressing MDR1 (MDCK-MDR1) (2) kindly provided by the Netherland Cancer Institute (NKI-AVL). The MDCK cells form monolayers on membranes in trans-well plates. Compounds were run at 1 μM in the MDCK assay. Permeation of the test compounds from A to B direction and B to A was determined over a 90-minute incubation at 37°C and 5% CO_2 with a relative humidity of 95%. Efflux ratio is defined as:

ER = $Papp_{B\text{-}A}/Papp_{A\text{-}B}$.

AZ31 P_{app}: 5.94 (1E-6 cm/s) Efflux ratio: 7.28

AZ32 P_{app}: 33.7 (1E-6 cm/s) Efflux ratio: 0.41

Brain slice measurement. The fraction of unbound drug in brain (fu_{brain}) was determined using the rat brain slice binding method (3,4).

Rat brain slice binding: AZ31 (fu_{brain}): 0.125

AZ32 (fu_{brain}): 0.059

Plasma Protein Binding measurement. Rat plasma protein binding (fu_{plasma}) was determined by equilibrium dialysis (18 hrs) at 20 μM.

Mouse plasma protein binding: AZ31 (fu_{plasma}): 0.28

AZ32 (fu_{plasma}): 0.148

Mouse Brain PK. AZ32 was dosed at 200 mg/kg in HPMC/Tween formulation in healthy female Swiss athymic nu/nu mice and healthy C57bl6 mice. AZ31 was dosed at 100 mg/kg in propylene glycol formulation in healthy male CD1 mice.

AZ31 Kpuu = 0.03 (based on AUC data)

AZ32 Kpuu = 0.26 (based on AUC data)

Supplementary Figures

A

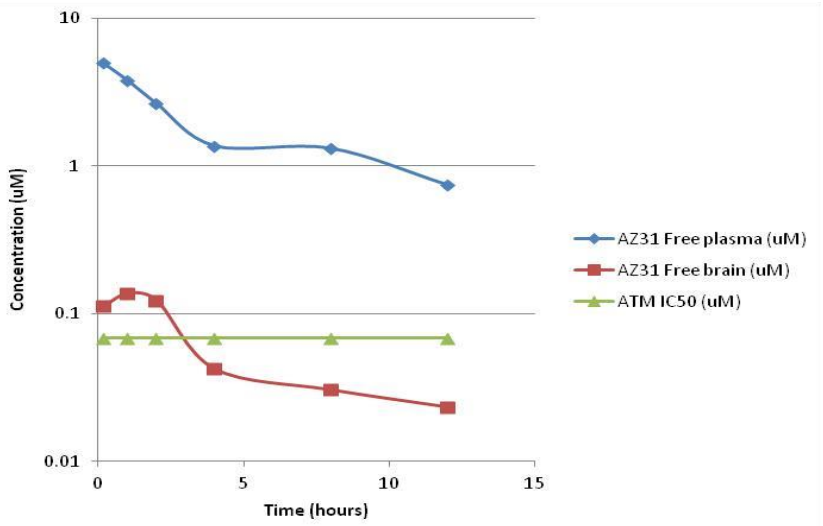

B

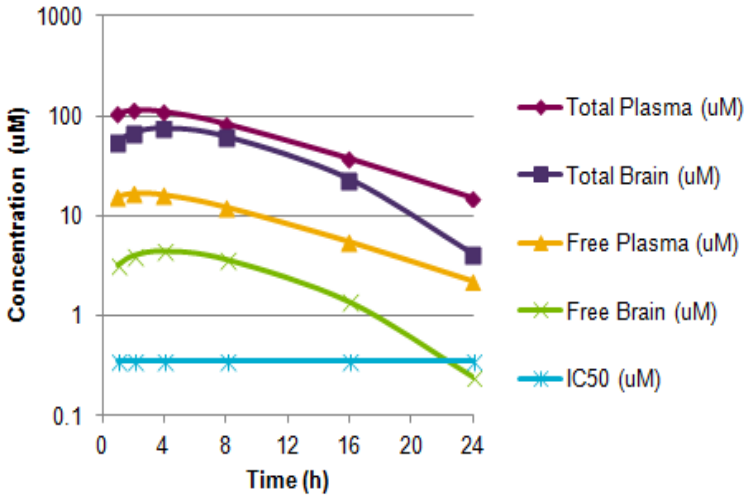

Supplementary Figure S1. Pharmacokinetic profiles of AZ31 and AZ32 in mouse. **A,** Free plasma versus free brain concentrations of AZ31 (100 mg/kg p.o.) in mouse. Plasma exposure achieved for a predicted 24 hrs cover over the cellular IC_{50} of ATM inhibition. Brain exposure is achieved for just 3 hrs over IC_{50}. **B,** Pharmacokinetic profiles of AZ32 in mouse. Pharmacokinetic plasma and brain concentrations of AZ32 in mouse dosed at 200 mg/kg p.o, giving free brain exposures over ATM cell IC_{50} for 22 hours.

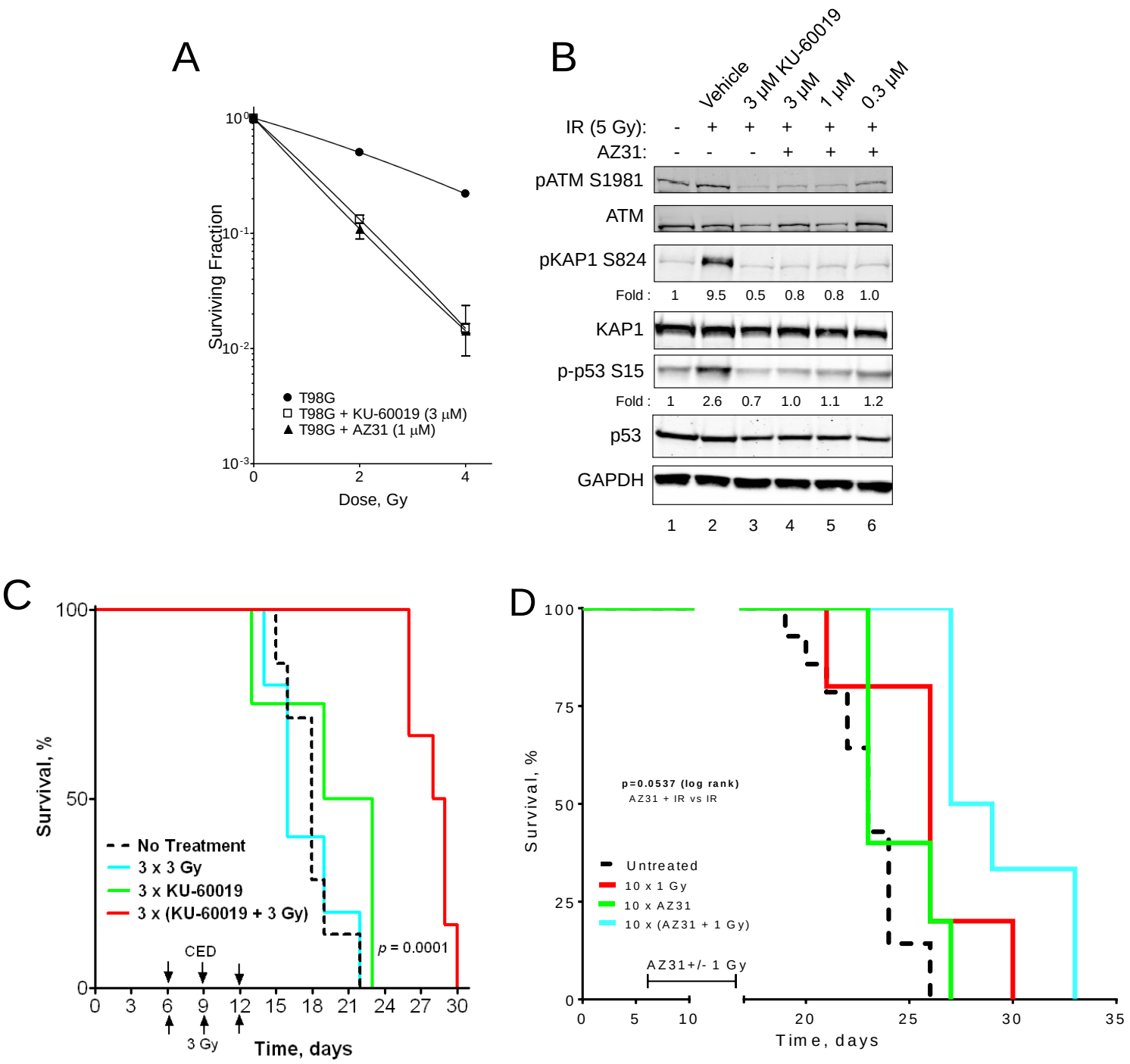

Supplementary Figure S2. ATM kinase inhibitor AZ31 radiosensitizes human glioma cells and inhibits the DDR. **A,** Human glioma T98G (p53 mutant) cells were plated as single cells on 6-cm dishes at appropriate numbers depending on radiation dose. After allowing the cells to attach (3-4 h), the cells were treated with 3 μM KU-60019 or 1 μM AZ31 for 1 h prior to irradiation. The cells were irradiated at the dose given and placed in a humidified CO_2 incubator over-night. The following morning, the medium was changed and the colonies formed over 10-14 days. The colonies were fixed/stained with 0.2% crystal

violet solution (in 20% MeOH) and counted. **B,** ATM kinase inhibitor AZ31 blocks the DDR in human glioma cells. T98G cells treated with KU-60019 (3 μM) or AZ31 at the indicated concentration for 1 h, followed by 5 Gy irradiation, then harvested ~10-15 min later. Samples were separated on a 7.5% gel and transferred to nitrocellulose and exposed to the indicated antibodies. **C,** KU-60019 radiosensitizes intra-cranial mouse glioma in immune-competent mice. Mouse GL261 (p53-153P) tumors grown in C57bl/6 mice are radiosensitized by KU-60019 administered by convection-enhanced delivery (CED) immediately prior to radiation. **D,** AZ31 treatment barely radiosensitizes intra-cranial mouse glioma in immune-competent mice. Mouse GL261 tumors grown in C57bl/6 mice were irradiated daily for 2 week with whole-head 137-Cs (1 Gy). AZ31 (100 mg/kg; p.o. QD) administration by oral gavage preceeding radiation by 1 hr. Mice were euthanized when moribund which occurred for Untreated (23 ± 1 day); 10 x 1 Gy (26 ± 1 day); 10 x AZ31 (24 ± 1 day); 10 x AZ31 + 1 Gy (29 ± 1 day). p (log-rank) = 0.0537.

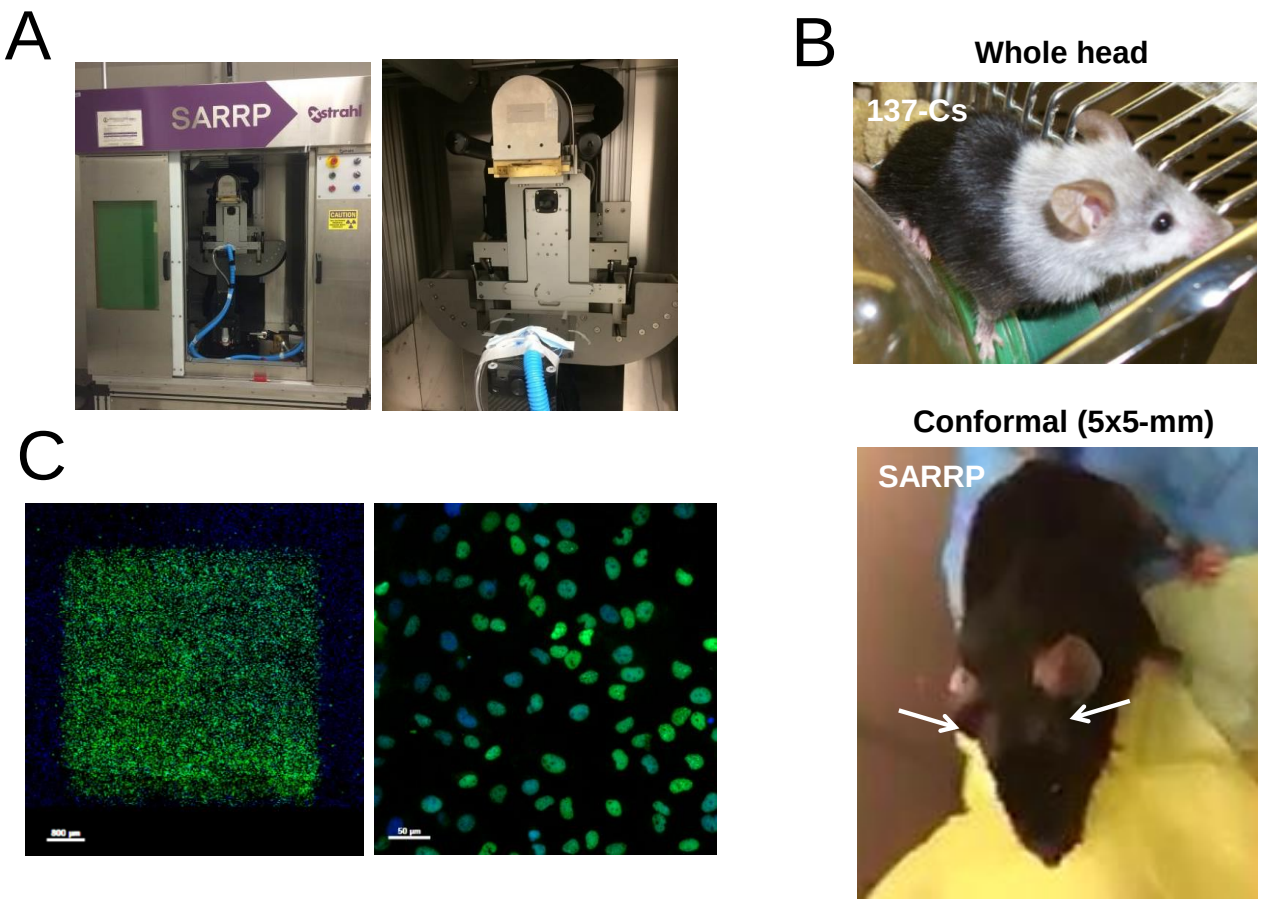

Supplementary Figure S3. SARRP irradiation reduces radiation-induced toxicity. **A,** SARRP is a small animal radiation research platform, combining cone beam CT imaging with a micro irradiation system – using SARRP will avoid irradiating the salivary glands. **B,** AZ32 and 137-Cs whole-head irradiation causes mucositis (?) (difficulties eating and drinking). Hair-follicles are sensitive to radiation resulting in whitening of fur. The images show whole head and conformal areas where radiation resulted in whitening of fur. **C,** Precise SARRP (5 x 5-mm) irradiation (5 Gy) of U1242 glioma cells grown on a chamber slide. Cells were fixed 1 hr after irradiation and exposed to rabbit anti - γ-H2AX antibody followed by goat anti-rabbit-AlexaFluor-488 and DAPI. The slide was scanned using the Vectra® Polaris™ Automated Quantitative Pathology Imaging System. Size bars depict 800 (*left*) and 50 (*right*) μm, respectively.

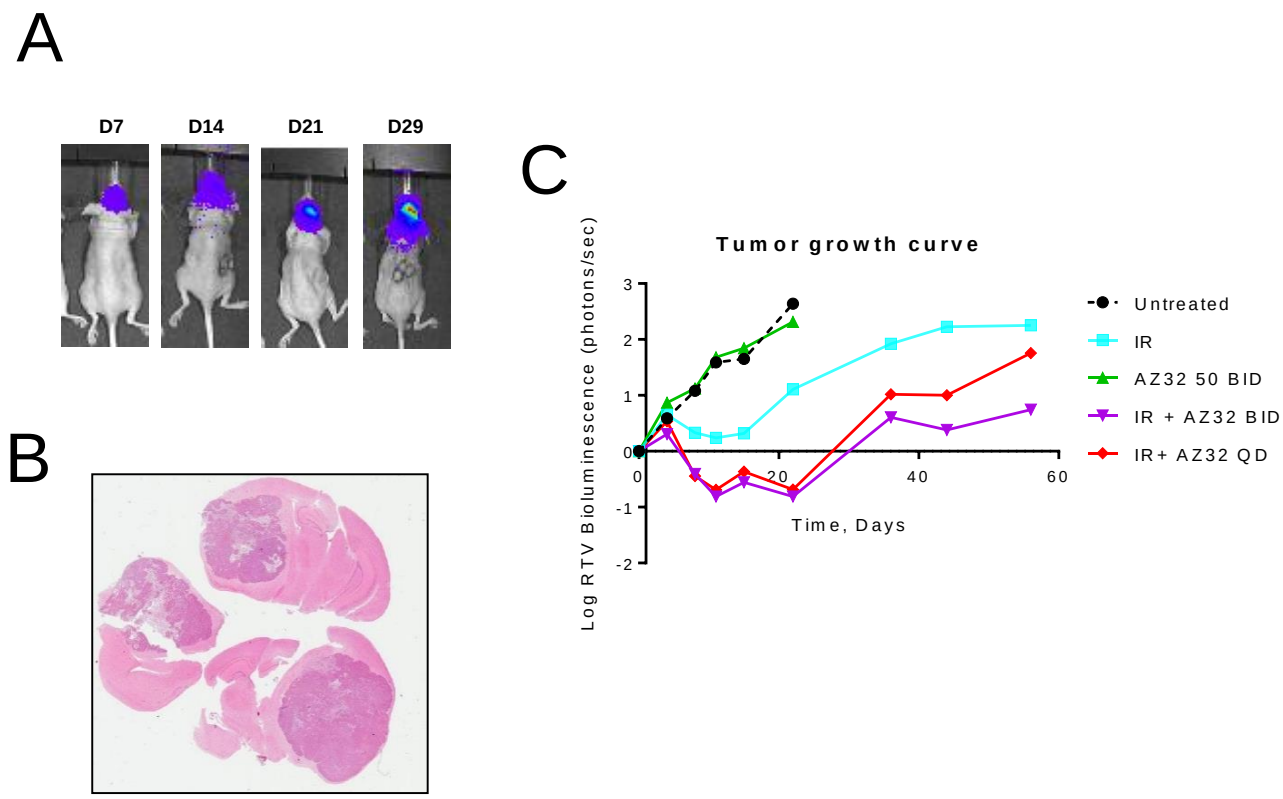

Supplementary Figure S4. Brain NCI-H2228 non-small cell lung cancer brain mets are radiosensitized by AZ32. **A,** Tumor growth in brain was measured by Xenogen-IVIS-200 imaging system from start of treatment and assessed by the mean change in BLI intensity. **B,** Tumor was confirmed by histological assessment. **C,** AZ32 and radiation groups showed a significant improved survival compared to radiation alone group.

A

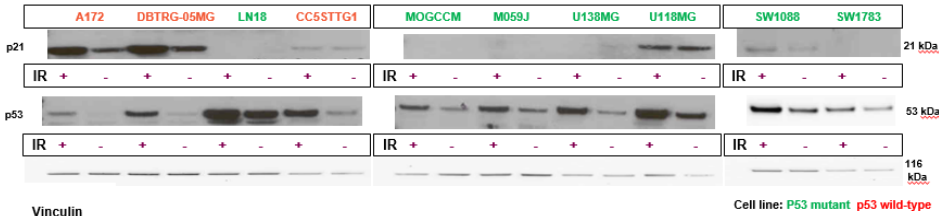

B

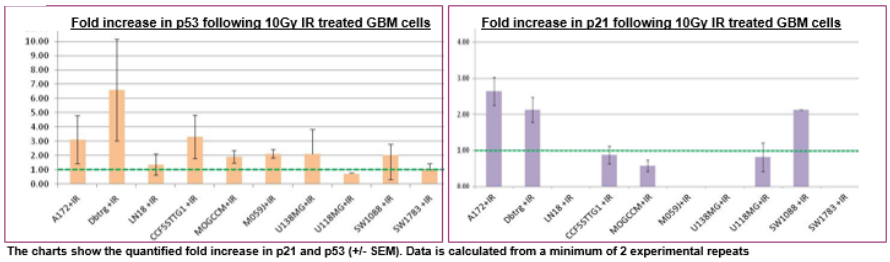

The charts show the quantified fold increase in p21 and p53 (+/- SEM). Data is calculated from a minimum of 2 experimental repeats

C

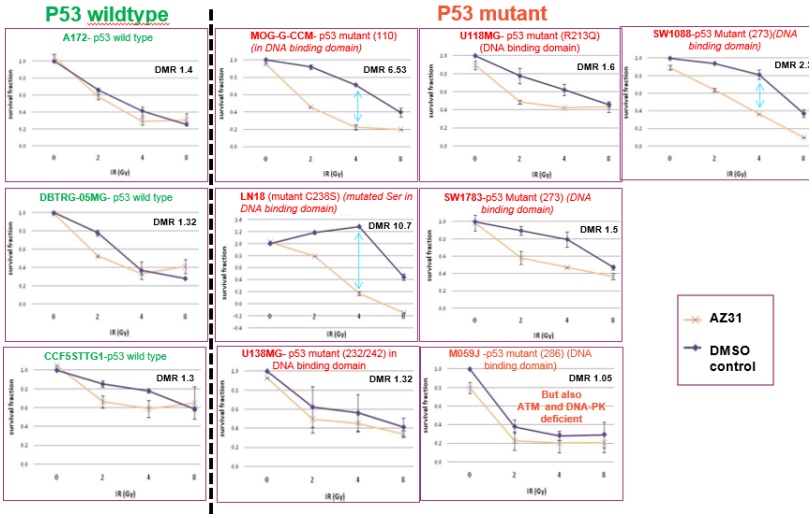

D

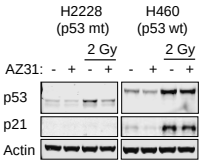

E

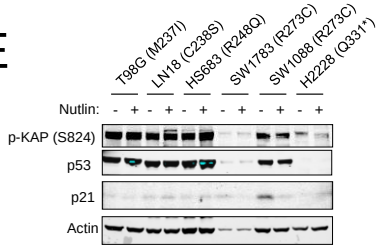

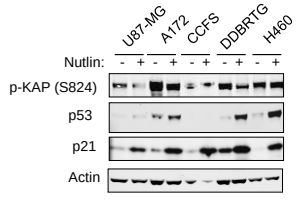

F

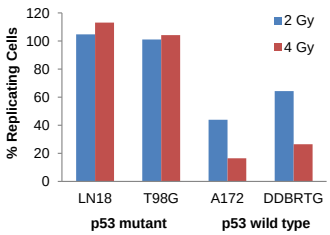

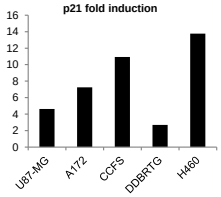

Supplementary Figure S5. p53 functionality assays. **A,** Western blotting of p53 and p21 after radiation with 10 Gy. Samples collected at 24 hr post-irradiation. Vinculin was used to normalize loading. **B,** Summary of p53 and p21 induction levels. Quantification of p53 and p21 protein levels by western blotting (n = 3) obtained from (A) was plotted as folds. The result was incorporated into **Table 2**. **C,** Dose modifying ratios (DMR) of irradiated GBM cell lines with or without AZ31. Representative examples of radiosensitization survival curves across the GBM cell line panel. Average DMR (n=3) is shown in **Table 2**. Cells were seeded in 384-well plates and dosed with AZ31 (1 μM) an hour before irradiation. Total cell counts were measured by Saponin and live cells measured by Sytox green at day 0 and day 5 after irradiation. DMR (fold radiosensitization achieved by AZ31) calculated after irradiation with 4 Gy. **D,** p53 is not stabilized after radiation in lung cancer cells with mutant p53 (H2228), unlike wild-type cells (H460). AZ31 (10 nM) further destabilizes mutant p53 but not wild-type, after radiation. **E,** GBM and lung cancer cells with mutant p53 (*top*), unlike wild-type (*middle*), cells have high basal levels of p53 and are unable to induce p21 by Nutlin (1 μM) (activates p53 via the prevention of MDM2 degradation) whereas wild-type cells induce p21 2-12 fold (*bottom*). **F,** GBM cells with mutant p53, unlike wild-type cells, have defective radiation-induced G1/S checkpoint and show unabated replication after radiation.

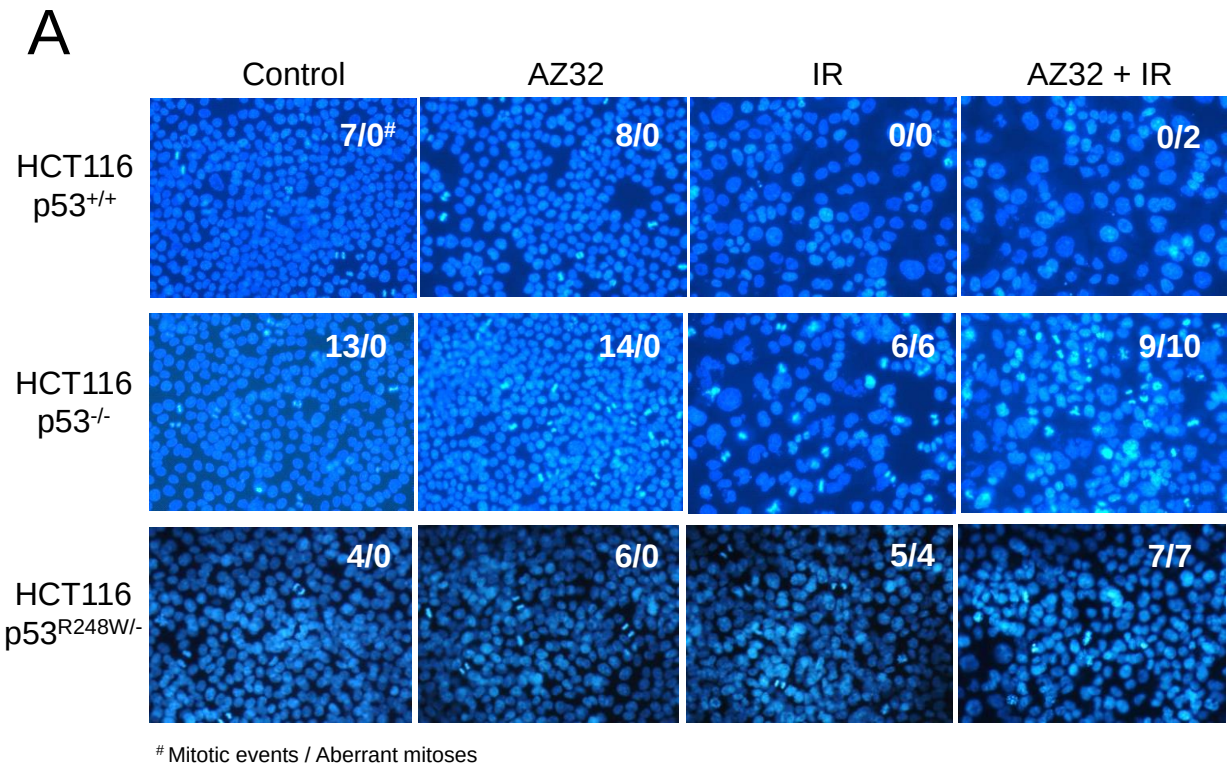

Mitotic events / Aberrant mitoses

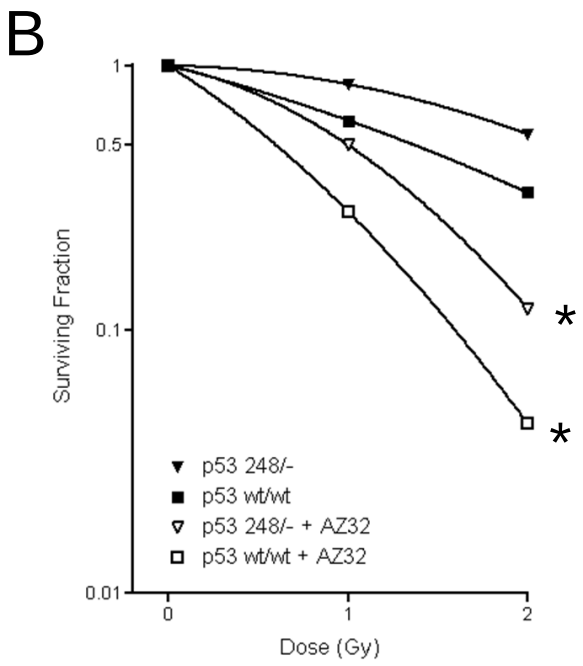

Supplementary Figure S6. Enhanced mitotic catastrophe in HCT116 p53 null/mutant cells after exposure to AZ32 and radiation. **A,** HCT116 p53$^{+/+}$, p53$^{-/-}$, and p53$^{R248W/-}$ cells (kindly provided by B. Vogelstein (5)) were treated with AZ32 (3 μM) or not, +/- 3 Gy, and 3 days later examined for normal and aberrant mitotic figures (inserted numerical values) by DAPI stain. Control -/- cells show a 2-fold (13/7) elevated mitotic index relative to +/+ cells

whereas irradiated +/+ cells have no mitotic events after IR indicative of impaired and intact G1/S and G2/M checkpoints, respectively. AZ32 alone showed increased aberrant mitoses (6/6) whereas +/+ cells had no mitosis nor aberrant ones. AZ32+IR of -/- cells show much higher frequency of aberrant mitotic figures and polyploidy cells than +/+ cells (compare 9/10 with 0/2) indicative of mitotic catastrophe. A similar result seen with HCT116 $p53^{-/-}$ cells was also observed with HCT116 $p53^{R248W/-}$ cells. **B,** ATMi radiosensitizes both wild type and p53 mutant HCT116 cells. Log plot of surviving fraction vs. radiation dose. Colony forming assay shows that treatment with AZ32 radiosensitizes both wild type and mutant p53 (R248W/-) cells. Wild type HCT116 cells are sensitized to a greater degree than p53 mutant cells. Survival reduction factors for wild type cells are 2.2 (1 Gy) and 7.5 (2 Gy). Survival reduction factors for the p53 (248/-) mutant cells are 1.7 (1 Gy) and 4.6 (2 Gy). At 2 Gy, +/-AZ32 for each of the two cell lines were statistically significant ($p < 0.05$).

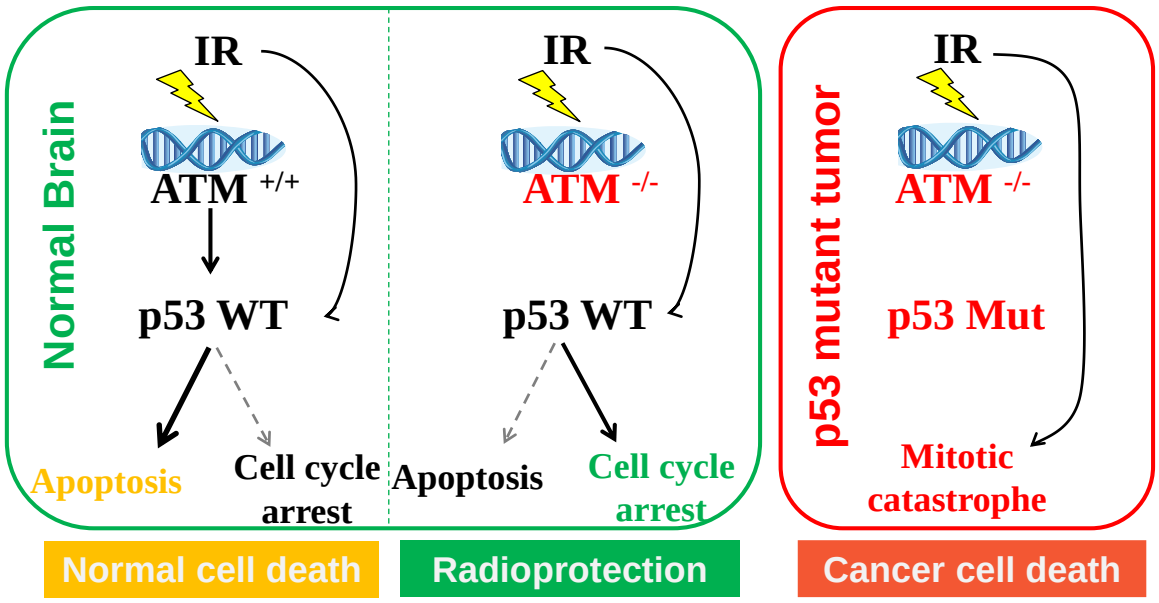

Supplementary Figure S7. Model for ATMi radiosensitization of mutant p53 gliomas and possible protection of normal healthy CNS. See text for discussion. ATM is required for p53-dependent, radiation-induced neuronal apoptosis in the mouse (6). Thus, transient ATMi CNS exposure might not be toxic and in fact could protect against neuronal cell death if provided post-irradiation.

GBM cell line	p53 status	DER
LN18	C238S	5.8
U1242	R175H	3.0
T98G	M237I	2.3
DBTRG	Wild-type	1.8
U87MG	Wild-type	1.7

Supplementary Table 1. Dose enhancement ratios of radiosurvival curves shown in Fig. 1A. Dose enhancement ratio (DER) was calculated from the survival curves as the ratio of survival values without and with AZ32 at 2 Gy.

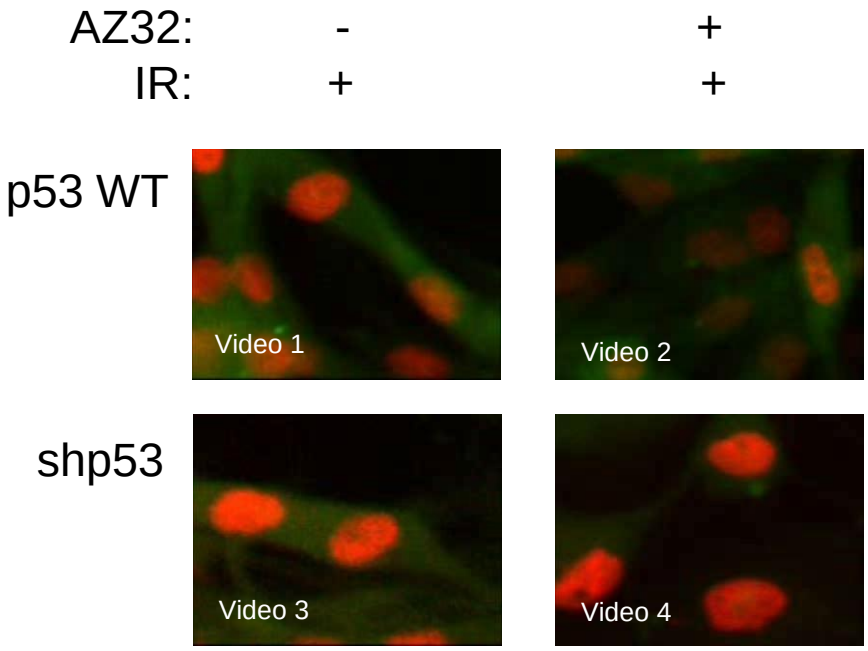

Supplementary Video S1-S4. ATMi increases the rate of mitotic catastrophe in glioma cells when p53 is knocked down. U87/puro (*p53 WT*) and U87/shp53 (*shp53*) were seeded on dishes with cover slip bottoms, treated with or without AZ32 (3 μM), and irradiated (5 Gy). Time-lapse videos were recorded intermittently (every 7 min) over 16 hrs. Time series of mitosis in U87/Centrin2-EGFP/H2B-mCherry and U87/shp53/Centrin2-EGFP/H2B-mCherry cells. Treatment with AZ32 does not appear to greatly increase the frequency of aberrant mitoses in p53 wild type cells, but does so in shp53 cells.

References

1. Degorce SL, Barlaam B, Cadogan E, Dishington A, Ducray R, Glossop SC*, et al.* Discovery of Novel 3-Quinoline Carboxamides as Potent, Selective, and Orally Bioavailable Inhibitors of Ataxia Telangiectasia Mutated (ATM) Kinase. Journal of medicinal chemistry **2016**;59(13):6281-92.
2. Pastan I, Gottesman MM, Ueda K, Lovelace E, Rutherford AV, Willingham MC. A retrovirus carrying an MDR1 cDNA confers multidrug resistance and polarized expression of P-glycoprotein in MDCK cells. Proceedings of the National Academy of Sciences of the United States of America **1988**;85(12):4486-90.
3. Friden M, Bergstrom F, Wan H, Rehngren M, Ahlin G, Hammarlund-Udenaes M*, et al.* Measurement of unbound drug exposure in brain: modeling of pH partitioning explains diverging results between the brain slice and brain homogenate methods. Drug Metab Dispos **2011**;39(3):353-62 doi 10.1124/dmd.110.035998.
4. Di L, Umland JP, Chang G, Huang Y, Lin Z, Scott DO*, et al.* Species independence in brain tissue binding using brain homogenates. Drug Metab Dispos **2011**;39(7):1270-7 doi 10.1124/dmd.111.038778.
5. Sur S, Pagliarini R, Bunz F, Rago C, Diaz LA, Jr., Kinzler KW*, et al.* A panel of isogenic human cancer cells suggests a therapeutic approach for cancers with inactivated p53. Proceedings of the National Academy of Sciences of the United States of America **2009**;106(10):3964-9.
6. Herzog KH, Chong MJ, Kapsetaki M, Morgan JI, McKinnon PJ. Requirement for Atm in ionizing radiation-induced cell death in the developing central nervous system. Science **1998**;280(5366):1089-91.